JACS
JOURNAL OF THE AMERICAN CHEMICAL SOCIETY

Article

pubs.acs.org/JACS

Fluorescent Neuraminidase Assay Based on Supramolecular Dye Capture After Enzymatic Cleavage

Wenqi Liu, César F. A. Gómez-Durán, and Bradley D. Smith*

Department of Chemistry and Biochemistry, University of Notre Dame, 236 Nieuwland Science Hall, Notre Dame, Indiana 46556, United States

Supporting Information

ABSTRACT: A conceptually new type of enzymatic cleavage assay is reported that utilizes in situ supramolecular capture of the fluorescent product. A squaraine-derived substrate with large blocking groups at each end of its structure cannot be threaded by a tetralactam macrocycle until the blocking groups are removed by enzyme cleavage. A prototype design responds to viral neuraminidase, an indicator of influenza infection, and also measures susceptibility of the sample to neuraminidase inhibitor drugs. The substrate structure incorporates three key features: (a) a bis(4-amino-3-hydroxyphenyl)squaraine core with bright deep-red fluorescence and excellent photostability, (b) an *N*-methyl group at each end of the squaraine core that ensures fast macrocycle threading kinetics, and (c) sialic acid blocking groups that prevent macrocycle threading until they are removed by viral neuraminidase. The enzyme assay can be conducted in aqueous solution where dramatic colorimetric and fluorescence changes are easily observed by the naked eye. Alternatively, affinity capture beads coated with macrocycle can be used to immobilize the liberated squaraine and enable a range of heterogeneous analysis options. With further optimization, this new type of neuraminidase assay may be useful in a point of care clinic to rapidly diagnose influenza infection and also determine which of the approved antiviral inhibitor drugs is likely to be the most effective treatment for an individual patient. The assay design is generalizable and can be readily modified to monitor virtually any type of enzyme-catalyzed cleavage reaction.

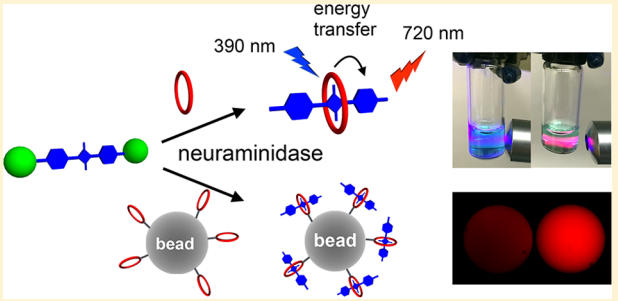

INTRODUCTION

Enzyme assays are ubiquitous in modern society. They are employed extensively as laboratory tools in basic biomedical research, drug discovery, food technology, and pollution control.[1−3] In addition, a range of diagnostic devices are used to monitor enzymes that affect public health, personal well-being, and environmental protection.[4−6] The high sensitivity of fluorescence makes it an especially powerful technique, and ongoing innovations in photonics engineering such as microfluidic chips,[7,8] CCD cameras for multiplex detection,[9,10] and benchtop flow cytometers[11] offer new opportunities to greatly enhance assay performance properties such as limit of detection, spatiotemporal resolution, and sample throughput.[12,13] Successful exploitation of the new instrumentation requires concomitant improvements in fluorescence assay design.[14−16] An enzyme is a catalyst, thus the fluorescence signal in a cleavage assay continues to build up over time. But the cleavage product diffuses throughout the entire volume of the assay sample which dilutes the fluorescence signal. Moreover, the signal-to-background ratio is further lowered in turbid samples due to scattering of the light. In principle, the sensitivity of a substrate cleavage assay would be enhanced if the liberated fluorescent product was sequestered by affinity capture beads.[17] Furthermore, product immobilization provides access to a suite of automated heterogeneous analysis methods.[18] Surprisingly, there has been very little exploration of assays that incorporate in situ capture of the cleaved product,[18−21] and essentially no reports of a cleavage assay that captures and concentrates a liberated dye.[22] One reason for this circumstance is the scarcity of supramolecular host molecules that have very high affinity for fluorescent dyes.[23] To be clear, there are enzyme assays that use dye displacement from metal cations[24] or container molecules such as cyclodextrin or cucurbituril, but these systems do not immobilize the dye and permit spatially localized detection.[25−27]

We have recently developed a high-affinity self-assembly system that we call Synthavidin technology.[23,28−30] In short, a tetralactam macrocycle with anthracene sidewalls can be rapidly threaded by squaraine dyes in water to form very stable complexes with nanomolar dissociation constants. The threaded complexes are stabilized by four strong hydrogen bonds with the two squaraine oxygen atoms and hydrophobic stacking of aromatic surfaces. Squaraine dyes exhibit very intense deep-red absorption/emission bands, and macrocycle threading is indicated by three characteristic changes in photophysical properties: (a) red-shifted squaraine absorption/emission bands, (b) increased squaraine fluorescence

Received: February 15, 2017
Published: April 20, 2017

DOI: 10.1021/jacs.7b01628
J. Am. Chem. Soc. 2017, 139, 6390−6395

quantum yield, and (c) efficient energy transfer from the excited anthracene sidewalls to the encapsulated squaraine dye. In addition, the N-substituents at each end of the dye structure have little impact on the association constant but greatly affect the threading kinetics. When the dyes have *N*-propyl groups, the threading kinetics are relatively slow, and we have utilized this feature to produce a preassembly method that creates mechanically stable threaded complexes for long-term biological imaging.[31,32] In this current study we demonstrate for the first time how Synthavidin technology can be exploited for a very different purpose; that is, to create a new class of enzyme assays that utilize in situ capture of the fluorescent cleavage product. The basic concept is shown schematically in Scheme 1a. A squaraine dye with large blocking groups at each end of its structure cannot be threaded by a tetralactam macrocycle until the blocking groups are removed by enzymatic cleavage.

Scheme 1. (a) Enzyme Cleavage Assay Based on in Situ Dye Capture, (b) Molecular Structures Used in This Prototype Study for Detection of Neuraminidase, and (c) Structure of SQ2 Used in Preliminary Binding Studies[a]

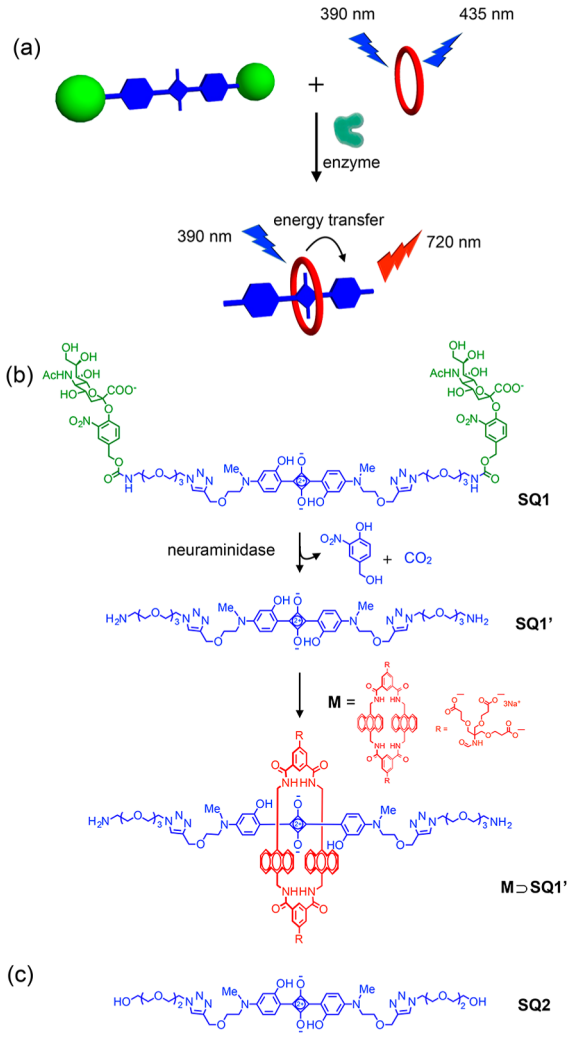

[a](a) A tetralactam macrocycle (red oval) encapsulates a fluorescent squaraine dye (blue) after enzymatic cleavage of the blocking groups (green). (b) Self-immolative cleavage of a sialic acid group releases a quinone methide that is rapidly trapped by water and also liberates SQ1′.

Scheme 1b,c shows the specific molecular structures used in the current study. The key compound is squaraine substrate **SQ1** which has several supramolecular and photophysical innovations. Guided by our previous experience, and some molecular modeling (Scheme S5), we chose a bis(4-amino-3-hydroxyphenyl)squaraine as the fluorescent core which was expected to be brighter and more photostable than the bis(2-aminothiophene)squaraine system that we had used in our earlier preassembly studies.[33,34] For reasons that are discussed in the next paragraph, the blocking groups in **SQ1** are sialic acid derivatives that prevent threading of macrocycle **M** until they are removed enzymatically. Self-immolative cleavage of the sialic acid groups liberates **SQ1′** which has an *N*-methyl group at each end of the squaraine core that allows rapid formation of **M** ⊃ **SQ1′**.

The functional aim of this prototype study was to develop an assay that responds to viral neuraminidase (VNA), an enzyme indicator of influenza infection.[35] Each year in the United Sates, around 5−15% of the population becomes infected with seasonal influenza, and there are approximately 25,000 influenza-associated deaths.[36,37] The morbidity and mortality increases dramatically during pandemics, such as the 2009 outbreak of swine flu, placing great strain on the global health care infrastructure. VNA cleaves *N*-acetylneuraminic acid (sialic acid) from the surface of host cells to release viral progeny[38,39] and is considered a prominent biomarker of contamination in biomedical and environmental samples.[35] Furthermore, assays that measure VNA activity can provide direct information about the likely efficacy of neuraminidase inhibitor drugs to treat the specific strain of influenza that infects an individual patient. The efficacy window for VNA inhibitor drugs is within 48 h of the onset of influenza; thus, there is a great need for low-cost and portable methods to rapidly confirm influenza infection. Most of the currently available rapid response tests are based on nucleic acid amplification tests or immunoassays directed at viral antigens.[40] The former requires sophisticated instruments or training, while the latter are often cost restricted. Other methods of neuraminidase detection include electrochemistry[41] or chemiluminescence[42] techniques that may be challenging to automate for high-throughput or multiplex testing. There are several neuraminidase cleavage assays that release a fluorescent dye,[43,44] but there is no example that captures and concentrates the liberated dye on a bead for facilitated analysis.

The project work flow was in three parts. First, the different molecular building blocks had to be prepared, and the self-assembly processes evaluated in aqueous solution to confirm that the supramolecular and photophysical properties were appropriate. Then the enzyme-triggered, dye capture process in Scheme 1 had to be validated. Finally, affinity capture beads coated with macrocycle **M** had to be prepared and used in an assay that determines if a specific strain of neuraminidase enzyme is susceptible to inhibition by a clinically relevant influenza drug.

RESULTS AND DISCUSSION

Preliminary Demonstration of Self-Assembly. Solution-state titration studies assessed the threading of **M** by **SQ2**, a close structural analogue of **SQ1′** whose easy preparation on a large scale permitted an extensive number of supramolecular measurements. We were pleased to observe strong and very rapid threading to form **M** ⊃ **SQ2** as indicated by measured values of $K_a = (5.8 \pm 1.3) \times 10^7\ M^{-1}$ and $k_{on} = (5.1 \pm 0.5) \times 10^8\ M^{-1}\ s^{-1}$ (Figure 1). When the concentration of both

DOI: 10.1021/jacs.7b01628
J. Am. Chem. Soc. 2017, 139, 6390−6395

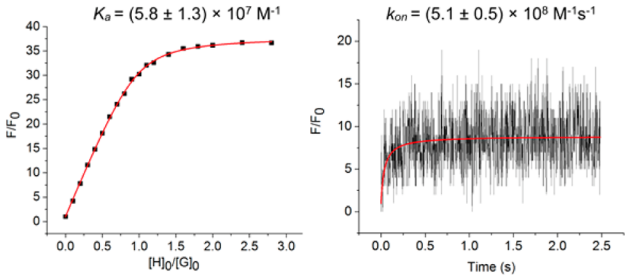

Figure 1. (left) Titration isotherm showing change in fluorescence for **SQ2** (250 nM) upon titration with **M** in water at 20 °C (ex: 680 nm, em: 695 nm). (right) Change in fluorescence over time (stopped-flow) for **SQ2** (50 nM) after addition of **M** (50 nM) in H_2O at 20 °C (ex: 680 nm, em: 695 nm).

partners (**M** and **SQ2**) was each 50 nM, bimolecular association was essentially complete within 300 ms, suggesting that squaraine threading by the macrocycle was not likely to become the rate-determining step in any putative enzyme cleavage assay. The threading of **SQ2** to form **M** ⊃ **SQ2** produced very favorable changes in squaraine photophysical properties (Table S1). Notably, there was a 39 nm red-shift in the squaraine emission wavelength and an increase in fluorescence quantum yield from 0.08 to 0.19. The combination of these changes meant that **SQ2** complexation by **M** produced a 35-fold enhancement in squaraine deep-red fluorescence intensity (ex: 680 nm, em: 695 nm). The **M** ⊃ **SQ2** complex exhibited a Stokes shift of 34 nm, which is very large for deep-red fluorescent dye.[45] A large Stokes shift is a desirable property because it minimizes dye self-quenching when the multiple copies are closely packed on the surface of an assay bead. There was also efficient energy transfer from the excited anthracene sidewalls in the surrounding macrocycle to the encapsulated squaraine dye (Figure S2). Another favorable property of **SQ2** and threaded complex **M** ⊃ **SQ2** is very high photostability as judged by the lack of photobleaching after long periods of constant irradiation (Figure S3). Taken together, these favorable supramolecular and photophysical results demonstrated the high feasibility of **M** and **SQ2** (or related analogues) as a self-assembly pair for in situ capture and fluorescence signaling after enzymatic cleavage of suitably designed squaraine blocking groups.

Solution-State Studies of Neuraminidase Triggered Formation of M ⊃ SQ1′. The sialic acid blocking groups on **SQ1** had to be large enough to prevent threading by **M** and also be cleaved by neuraminidase within an acceptable analysis time frame. The structure of **SQ1** included self-immolative linkers with the expectation that sialic acid hydrolysis would initiate a bond breaking cascade that liberated squaraine **SQ1′**.[8,46,47] This design feature was confirmed by ESI mass spectrometry experiments that analyzed samples of **SQ1** before and after treatment with bacterial neuraminidase (BNA) from *Clostridium perfringens*, a convenient neuraminidase for these preliminary studies.[48] As shown in Figure S4, the peak for **SQ1** was consumed after adding BNA and a peak corresponding to **SQ1′** was produced. Blocking group removal was also indicated by changes in the squaraine absorption and fluorescence spectra because the cleavage product **SQ1′** self-aggregates when it is free in water leading to absorption band broadening and fluorescence quenching (Figure S5).

Additional solution-state absorption and fluorescence studies confirmed the other necessary supramolecular features shown in Scheme 1. When **M** and **SQ1** were mixed together, there were very small changes in the squaraine absorption and emission spectra (Figures 2a,b) perhaps due to weak hydrophobic association of the two molecules. Subsequent addition of BNA to this mixture of **M** and **SQ1** triggered the expected 18 nm red-shift in the squaraine absorption maximum, along with large enhancements in the strongly red-shifted squaraine fluorescence emission, spectral changes that are highly consistent with BNA cleavage of the sialic acid blocking groups, followed by macrocycle threading to form **M** ⊃ **SQ1′**. The most compelling evidence for macrocycle threading was the enzyme-dependent enhancement in internal fluorescence energy transfer when the sample was excited by UV light. As shown in Figures 2c,d, there was a significant decrease in the macrocycle anthracene emission band and a corresponding large increase in deep-red fluorescence from the encapsulated squaraine. The fluorescence energy-transfer effect was easily observed by the naked eye as a dramatic change in sample emission color from blue to red when the vials were Illuminated with UV light from a hand-held lamp (Figure 2e) or a blue laser pointer (Figure 2f).

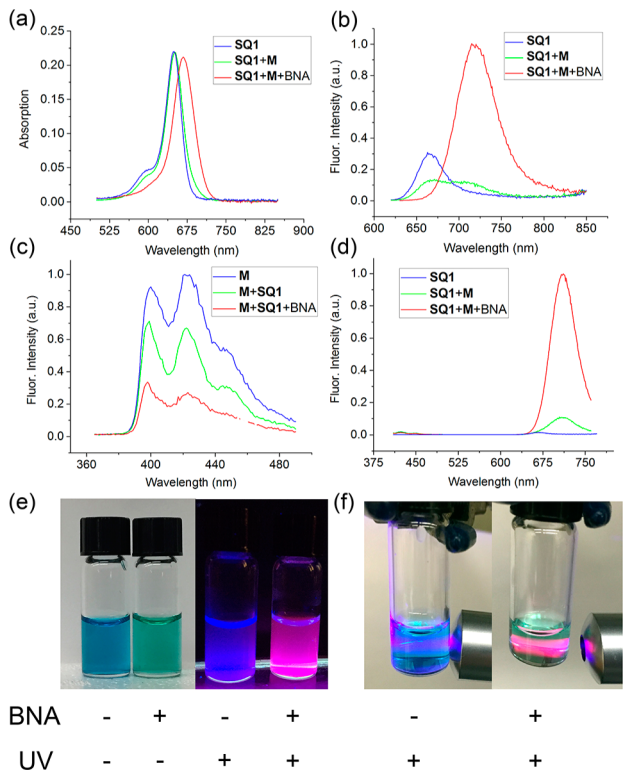

Figure 2. Optical evidence for the neuraminidase triggered self-assembly shown in Scheme 1. (a) Squaraine absorption band, (b) squaraine fluorescence (ex: 610 nm), (c) anthracene fluorescence (ex: 390 nm), (d) squaraine fluorescence after internal energy transfer from excited **M** (ex: 390 nm); for samples of **SQ1**, **SQ1** + **M**, and **SQ1** + **M** + BNA in water, where [**SQ1**] = [**M**] = 3 μM, [BNA] = 0.03 U per nmol^{-1} of substrate. Photographs of vials with illumination by laboratory light or: (e) portable UV lamp (ex: 365 nm, indicated by +), (f) blue laser pointer (ex: 410 nm, indicated by +). Each vial contained **SQ1** (20 μM) + **M** (40 μM), and the presence of BNA (0.03 U nmol^{-1} substrate) is indicated by + .

To gauge the relative reactivity of **SQ1** as a substrate for neuraminidase, the rate of enzyme-catalyzed cleavage was compared to 4-methylumbelliferyl-*N*-acetyl-α-D-neuraminic

DOI: 10.1021/jacs.7b01628
J. Am. Chem. Soc. 2017, 139, 6390−6395

acid (4-MUNANA), a well-known fluorescent substrate that releases a green-emitting 4-methylumbelliferone (Scheme S6).[43] Experiments using BNA and the clinically relevant VNA from H1N1 influenza virus showed that in each case the enzyme reaction of **SQ1** is about 10 times slower than 4-MUNANA (Figures S7 and S8). As expected from known neuraminidase substrate structure/activity relationships,[49] the rate of VNA-catalyzed cleavage was slower than the cleavage catalyzed by BNA. Nonetheless, consumption of all **SQ1** was complete well within the designated 1 h analysis period using 0.1 unit (U) of VNA per nmol of **SQ1**.

Assay for Neuraminidase Detection and Drug Susceptibility. The basis of the neuraminidase detection and drug susceptibility assay is illustrated in Scheme 2. The

Scheme 2. Basis of Neuraminidase Drug Susceptibility Assay

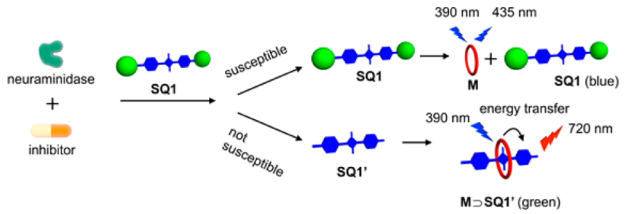

presence of active neuraminidase triggers cleavage of **SQ1** and formation of threaded **M** ⊃ **SQ1′** along with diagnostic spectral changes. These spectral changes are suppressed if the neuraminidase is inhibited by a drug. Initial studies were conducted in aqueous solution with the results shown in Figure 3. A microwell containing an admixture of **M** + **SQ1** was blue

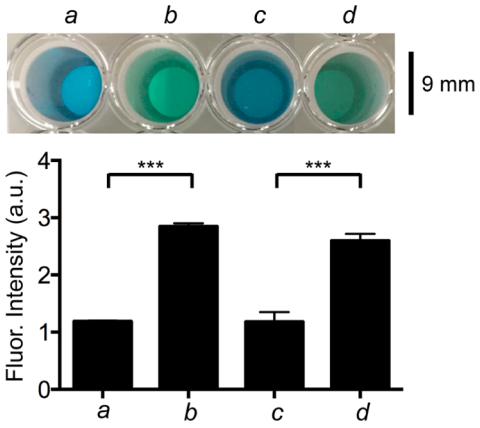

Figure 3. Solution-state version of the drug susceptibility test. (top) Photographs of four microwells containing aqueous solutions of: *a*, **SQ1** + **M**; *b*, **SQ1** + **M** + VNA; *c*, **SQ1** + **M** + VNA + Oseltamivir; *d*, **SQ1** + **M** + BNA + Oseltamivir. (bottom) Quantitative comparison of fluorescence intensity (ex: 620 nm, em: 725 nm) for each microwell, $N = 3$. (*** indicates p value <0.001).

to the naked eye (microwell *a*) and changed to green after the addition of VNA (microwell *b*). There was no color change when the VNA was inhibited by the drug Oseltamivir, a known inhibitor of VNA (microwell *c*). As expected, there was a color change to green when the admixture of **M** + **SQ1** + Oseltamivir was treated with BNA (microwell *d*) which is not inhibited by Oseltamivir.[50] These prototype results mimic the possible outcomes for a patient who is infected with a strain of flu containing neuraminidase that is either Oseltamivir-sensitive or Oseltamivir-resistant.

The next step was to demonstrate the bead-capture version of the assay that is illustrated conceptually in Figure 4. In this

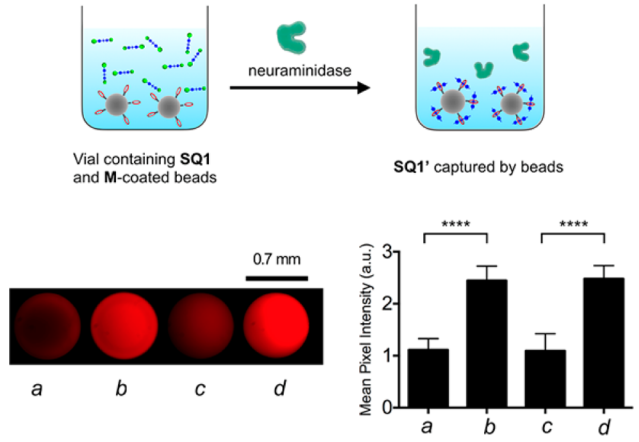

Figure 4. (top) Neuraminidase detection and drug susceptibility assay using **M**-coated beads to capture the **SQ1′** produced by enzymatic cleavage of **SQ1**. Each assay vial contained about 20 **M**-coated capture beads covered by a citrate solution containing: *a*, **SQ1**; *b*, **SQ1** + VNA; *c*, **SQ1** + VNA + Oseltamivir; *d*, **SQ1** + BNA + Oseltamivir. (bottom left) Deep-red micrographs (ex: 635–675 nm, em: 694–736 nm) showing a representative **M**-coated bead taken from the four separate assay vials. (bottom right) Average values of mean pixel intensity (MPI) for each set of 10 **M**-coated beads taken from the four separate assay vials (**** indicates p value <0.0001).

case, the cleavage product **SQ1′** was captured by beads coated with **M** and the individual beads subsequently interrogated using deep-red fluorescence microscopy. The **M**-coated beads were easily prepared by simply adsorbing the highly anionic **M** onto the surface of cationic Amberlite IRA-958 ion exchange beads (0.70 mm diameter). As shown in Figure S9, the **M**-coated beads exhibited strong UV/blue anthracene fluorescence that was readily apparent to the naked eye. Control experiments showed that the **M**-coated beads did not capture the blocked squaraine **SQ1** from aqueous solution, but there was obvious squaraine capture by the beads after **SQ1** was converted to **SQ1′**. The **M**-coated beads rapidly became blue to the naked eye, and fluorescence micrographs showed enhanced deep-red fluorescence intensity. Strong evidence that threaded **M** ⊃ **SQ1′** had formed on the bead surface was the observation of internal fluorescence energy transfer from excited **M** to **SQ1′** (Figure S10).

In the bottom left of Figure 4 are representative deep-red fluorescence micrographs of four individual **M**-coated beads, each one taken from a different assay vial. An individual assay vial started with about 20 **M**-coated capture beads, and at the end of the assay, 10 of these beads were removed for analysis using fluorescence microscopy (Figure S11). The bottom right of Figure 4 shows a graphical comparison of average fluorescence intensity for the four different sets of assay beads. The bead assay results matched the solution-state assay results above. That is, the presence of VNA produced a 2-fold increase in deep-red fluorescence from an **M**-coated bead due to capture of the deep-red fluorescent cleavage product **SQ1′**. The bead capture assay confirmed that Oseltamivir inhibited the added VNA (indicated by no change bead deep-red

DOI: 10.1021/jacs.7b01628
J. Am. Chem. Soc. 2017, 139, 6390–6395

fluorescence) but did not inhibit the added BNA (2-fold increase in bead fluorescence).

CONCLUSION

The results of this study are proof of concept for a novel fluorescent dye capture assay that detects enzymatic cleavage activity. The prototype design responds to viral neuraminidase, an indicator of influenza infection, and also measures susceptibility of the sample to neuraminidase inhibitor drugs. The assay is enabled by the extremely rapid and high affinity threading of tetralactam macrocycle **M** by squaraine dye **SQ1′** that is liberated after enzymatic cleavage of blocking groups from substrate **SQ1** (Scheme 1). The enzyme assay can be conducted in solution where the dramatic changes in optical properties can be easily detected by the naked eye (Figures 2 and 3). Alternatively, the assay can incorporate affinity capture beads to localize the liberated **SQ1′** which permits quantitative analysis by automated heterogeneous methods utilizing fluorescence microscopy, microarrays, microfluidics, or flow cytometry.[7−13,18] These methods can rapidly analyze large numbers of individual beads with great precision using cheap cameras and detectors. In addition, bead capture can increase detection sensitivity by removing the liberated dye from turbid samples (which lowers the background signal) and concentrating all of the dye within the interrogation volume of a focused excitation beam (which maximizes dye signal). With further optimization, this new type of fluorescent neuraminidase assay may be useful in a point of care clinic to immediately determine which of the two currently approved antiviral inhibitor drugs, Oseltamivir (Tamiflu) or Zanamivir (Relenza), is likely to be the most effective treatment for an individual patient. A portable and rapid test for the presence of influenza would improve patient treatment and reduce overuse of antivirals. Another important clinical analysis goal is to differentiate between the different classes of mammalian, bacterial and viral neuraminidase, and it should be possible to fine-tune the chemical structure of the sialic acid blocking groups in **SQ1** and achieve high specificity for influenza VNA.[49,50]

While this study focused only on fluorescence detection, it is worth emphasizing that squaraine dyes have structural features that enable high-sensitivity detection using other techniques such as electrochemistry,[51] electrogenerated chemiluminescence,[52] or surface enhanced resonance raman spectroscopy.[53] In addition, it should be straightforward to modify the design of this in situ squaraine capture assay and monitor a wide range of cleavage enzymes such as glycosidases, proteases, phosphatases, lipases, etc. Each case requires the enzyme to remove a blocking group from a suitably designed squaraine dye to allow release of **SQ1′** (or structural analogue) and subsequent solution-state capture by **M** or immobilization by **M**-coated beads. The growing literature on enzyme-triggered self-immolative bond cleavage processes will guide future efforts to create these new classes of squaraine substrates.[47,54]

EXPERIMENTAL SECTION

Detailed synthetic procedures and compound characterization are provided in the Supporting Information.

Solution-State Assay for Neuraminidase Activity and Drug Susceptibility. Appropriate aliquots were delivered to a microwell to give a 50 μL solution with the following concentrations: Oseltamivir (10 ng/μL), neuraminidase (VNA, 0.24 U/μL or BNA, 0.24 mU/μL), and **M** (0.8 mM), and the mixture incubated at room temperature for 30 min. **SQ1** (33 μL, 600 μM) was added, and the resulting solution was diluted to 100 μL and incubated for 1 h at 37 °C. A 10 μL aliquot of each microwell solution was transferred to 1 mL H_2O, the single point fluorescence intensity was measured (ex: 620 nm, em: 725 nm), and the average intensity was plotted on a bar graph with error bars corresponding to the standard deviation.

Preparation of M-Coated Beads. The macrocycle **M** (2 mg) and Amberlite IRA-958(Cl^-) ion exchange beads (Alfa Aesar, average diameter 0.70 mm) (300 mg) were mixed together in H_2O (1 mL), and the mixture shaken at room temperature for 30 min. The beads were filtered by centrifugation and washed with H_2O (6 × 3 mL).

Bead-Capture Assay for Neuraminidase Activity and Drug Susceptibility. Appropriate aliquots were delivered to a vial to give 140 μL solution with the following final concentrations: Sodium citrate (143 mM), enzyme (VNA, 0.09 U/μL or BNA, 0.09 mU/μL), and Oseltamivir (3.6 ng/μL) and incubated at room temperature for 30 min. **SQ1** (60 μL, 1 mM) and about 20 **M**-coated beads were added to the vials, and the mixture incubated for 1 h at room temperature. The beads were removed, washed with H_2O (6 × 3 mL), and imaged by fluorescence microscopy at 10× magnification on a Zeiss Axiovert 100 TV epifluoresence microscope equipped with an X-cite 120 fluorescence illumination system. Images of 10 separate beads taken from the same assay vial were acquired using an Andor iXon3 EMCCD camera operating in CCD mode with 20 ms acquisition time and a Cy5.5 filter set (ex: 635−675 nm, em: 694−736 nm) or a UV-Red filter set (ex: 352−402 nm, em: 694−736 nm). The fluorescence mean pixel intensity (MPI) for each bead micrograph was measured after using ImageJ software to draw a region of interest around the bead image. The average MPI for each set of 10 beads taken from a specific assay vial was plotted on a bar graph with error bars corresponding to the standard deviation.

ASSOCIATED CONTENT

Supporting Information

The Supporting Information is available free of charge on the ACS Publications website at DOI: 10.1021/jacs.7b01628.

Synthetic procedures, compound characterization and spectral data, experimental methods, and additional assay data (PDF)

AUTHOR INFORMATION

Corresponding Author

*smith.115@nd.edu

ORCID

Bradley D. Smith: 0000-0003-4120-3210

Notes

The authors declare no competing financial interest.

ACKNOWLEDGMENTS

This work was supported by grants from the NSF (CHE1401783), the University of Notre Dame Center for Advanced Diagnostics and Therapeutics, and the CONACyT (Mexico). We thank Scott Shaw for valuable assistance with fluorescence microscopy and analysis.

REFERENCES

(1) Reymond, J.; Fluxa, V. S.; Maillard, N. *Chem. Commun.* **2009**, *34*.

(2) Stauffer, C. E. *Enzyme Assays for Food Scientists*; Van Nostrand Reinhold: New York, 1989.

(3) Heery, B.; Briciu-Burghina, C.; Zhang, D.; Duffy, G.; Brabazon, D.; O'Connor, N.; Regan, F. *Talanta* **2016**, *148*, 75.

(4) Zhang, J.; Xiang, Y.; Wang, M.; Basu, A.; Lu, Y. *Angew. Chem., Int. Ed.* **2016**, *55*, 732.

(5) Burns, R. G.; DeForest, J. L.; Marxsen, J.; Sinsabaugh, R. L.; Stromberger, M. E.; Wallenstein, M. D.; Weintraub, M. N.; Zopini, A. *Soil Biol. Biochem.* **2013**, *58*, 216.

DOI: 10.1021/jacs.7b01628
J. Am. Chem. Soc. 2017, 139, 6390−6395

(6) Goddard, J. P.; Reymond, J. L. *Curr. Opin. Biotechnol.* **2004**, *15*, 314.
(7) Sjostrom, S. L.; Bai, Y.; Huang, M.; Liu, Z.; Nielsen, J.; Joensson, H. N.; Andersson Svahn, H. *Lab Chip* **2014**, *14*, 806.
(8) Thom, N. K.; Lewis, G. G.; Yeung, K.; Phillips, S. T. *RSC Adv.* **2014**, *4*, 1334.
(9) Yoo, S. M.; Lee, S. Y. *Trends Biotechnol.* **2016**, *34*, 7.
(10) Prakash, R.; Pabbaraju, K.; Wong, S.; Wong, A.; Tellier, R.; Kaler, K. V. I. S. *Micromachines* **2015**, *6*, 63.
(11) Czeh, A.; Schwartz, A.; Mandy, F.; Szoke, Z.; Koszegi, B.; Feher-Toth, S.; Nagyeri, G.; Jakso, P.; Katona, R. L.; Kemeny, A.; Woth, G.; Lustyik, G. *Cytometry, Part A* **2013**, *83*, 1073.
(12) Hertzberg, R. P.; Pope, A. J. *Curr. Opin. Chem. Biol.* **2000**, *4*, 445.
(13) Casas-Godoy, L.; Sandoval, G. *Comb. Chem. High Throughput Screening* **2016**, *19*, 636.
(14) de la Rica, R.; Aili, D.; Stevens, M. M. *Adv. Drug Delivery Rev.* **2012**, *64*, 967.
(15) Ghale, G.; Nau, W. M. *Acc. Chem. Res.* **2014**, *47*, 2150.
(16) Othman, A.; Karimi, A.; Andreescu, S. *J. Mater. Chem. B* **2016**, *4*, 7178.
(17) Under linear Beer−Lambert conditions, fluorescence detection sensitivity is proportional to the concentration of dye in the optical path. A common method to increase detection sensitivity is to incorporate an amplification cycle into the assay and increase the molar amount of dye in the same volume (see: Scrimin, P.; Prins, L. J. *Chem. Soc. Rev.* **2011**, *40*, 4488). Dye capture is a fundamentally different way to enhance sensitivity, in that it increases dye concentration by reducing the volume.
(18) Pei, X.; Zhang, B.; Tang, J.; Liu, B.; Lai, W.; Tang, D. *Anal. Chim. Acta* **2013**, *758*, 1.
(19) Lévêque, C.; Ferracci, G.; Maulet, Y.; Grand-Masson, C.; Blanchard, M. P.; Seagar, M.; Far, O. E. *Biosens. Bioelectron.* **2013**, *49*, 276.
(20) Glickman, J. F.; Schmid, A.; Ferrand, S. *Assay Drug Dev. Technol.* **2008**, *6*, 433.
(21) Lopez, A.; Lovato, F.; Hwan Oh, S.; Lai, Y. H.; Filbrun, S.; Driskell, E. A.; Driskell, J. D. *Talanta* **2016**, *146*, 388.
(22) Ma, F.; Fischer, M.; Han, Y.; Withers, S. G.; Feng, Y.; Yang, G. Y. *Anal. Chem.* **2016**, *88*, 8587.
(23) Liu, W.; Samanta, S. K.; Smith, B. D.; Isaacs, L. *Chem. Soc. Rev.* **2017**, DOI: 10.1039/C7CS00011A.
(24) Severin, K. *Curr. Opin. Chem. Biol.* **2010**, *14*, 737.
(25) Dsouza, R. N.; Hennig, A.; Nau, W. M. *Chem. - Eur. J.* **2012**, *18*, 3444.
(26) Biedermann, S. F.; Nau, W. M.; Biedermann, F.; Hathazi, D. *Chem. Commun.* **2015**, *51*, 4977.
(27) You, L.; Zha, D.; Anslyn, E. V. *Chem. Rev.* **2015**, *115*, 7840.
(28) Peck, E. M.; Liu, W.; Spence, G. T.; Shaw, S. K.; Davis, A. P.; Destecroix, H.; Smith, B. D. *J. Am. Chem. Soc.* **2015**, *137*, 8668.
(29) Liu, W.; Peck, E. M.; Hendzel, K. D.; Smith, B. D. *Org. Lett.* **2015**, *17*, 5268.
(30) Smith, B. D. *Beilstein J. Org. Chem.* **2015**, *11*, 2540.
(31) Peck, E. M.; Battles, P. M.; Rice, D. R.; Roland, F. M.; Norquest, K. A.; Smith, B. D. *Bioconjugate Chem.* **2016**, *27*, 1400.
(32) Roland, F. M.; Peck, E. M.; Rice, D. R.; Smith, B. D. *Bioconjugate Chem.* **2017**, *28*, 1093.
(33) Collins, C. G.; Peck, E. M.; Kramer, P. J.; Smith, B. D. *Chem. Sci.* **2013**, *4*, 2557.
(34) Fu, N.; Gassensmith, J. J.; Smith, B. D. *Aust. J. Chem.* **2010**, *63*, 792.
(35) Turgeon, N.; Toulouse, M.-J.; Ho, J.; Li, D.; Duchaine, C. *Can. J. Microbiol.* **2017**, *63*, 119.
(36) Thompson, W. W.; Weintraub, E.; Dhankhar, P.; Cheng, P.-Y.; Brammer, L.; Meltzer, M. I.; Bresee, J. S.; Shay, D. K. *Influenza Other Respir. Viruses* **2009**, *3*, 37.
(37) Carlson, A. L.; Budd, A. P.; Perl, T. M. *Curr. Opin. Infect. Dis.* **2011**, *23*, 293.
(38) Air, G. M. *Influenza Other Respir. Viruses* **2012**, *6*, 245.
(39) von Itzstein, M. *Nat. Rev. Drug Discovery* **2007**, *6*, 967.
(40) Foo, H.; Dwyer, E. D. *Aust. Prescr.* **2009**, *32*, 64.
(41) Zhang, X.; Dhawane, A. N.; Sweeney, J.; He, Y.; Vasireddi, M.; Iyer, S. S. *Angew. Chem., Int. Ed.* **2015**, *54*, 5929.
(42) Buxton, R. C.; Edwards, B.; Juo, R. R.; Voyta, J. C.; Tisdale, M.; Bethell, R. C. *Anal. Biochem.* **2000**, *280*, 291.
(43) Okomo-Adhiambo, M.; Sheu, T. G.; Gubareva, L. V. *Influenza Other Respir. Viruses* **2013**, *7*, 44.
(44) Kurebayashi, Y.; Takahashi, T.; Otsubo, T.; Ikeda, K.; Takahashi, S.; Takano, M.; Agarikuchi, T.; Sato, T.; Matsuda, Y.; Minami, A.; Kanazawa, H.; Uchida, Y.; Saito, T.; Kawaoka, Y.; Yamada, T.; Kawamori, F.; Thomson, R.; von Itzstein, M.; Suzuki, T. *Sci. Rep.* **2015**, *4*, 4877.
(45) Escobedo, J. O.; Rusin, O.; Lim, S.; Strongin, R. M. *Curr. Opin. Chem. Biol.* **2010**, *14*, 64.
(46) Fernandes, A.; Viterisi, A.; Coutrot, F.; Potok, S.; Leigh, D. A.; Aucagne, V.; Papot, S. *Angew. Chem., Int. Ed.* **2009**, *48*, 6443.
(47) Alouane, A.; Labruere, R.; Le Saux, T.; Schmidt, F.; Jullien, L. *Angew. Chem., Int. Ed.* **2015**, *54*, 7492.
(48) Fujii, I.; Iwabuchi, Y.; Teshima, T.; Shibat, T.; Kikuchi, M. *Bioorg. Med. Chem.* **1993**, *1*, 147.
(49) Shimasaki, C. D.; Achyuthan, K. E.; Hansjergen, J. A.; Appleman, J. R. *Philos. Trans. R. Soc., B* **2001**, *356*, 1925.
(50) Holzer, C. T.; Vonitzstein, M.; Jin, B.; Pegg, M. S.; Stewart, W. P.; Wu, W. Y. *Glycoconjugate J.* **1993**, *10*, 40.
(51) Maltese, V.; Cospito, S.; Beneduci, A.; De Simone, B. C.; Russo, N.; Chidichimo, G.; Janssen, R. A. J. *Chem. - Eur. J.* **2016**, *22*, 10179.
(52) Zhang, L.; Fang, Y.-M.; Wang, R.-Y.; You, L.-X.; Fu, N.-Y.; Chen, G.-N.; Sun, J.-J. *Chem. Commun.* **2011**, *47*, 3855.
(53) Stokes, R. J.; Ingram, A.; Gallagher, J.; Armstrong, D. R.; Smith, W. E.; Graham, D. *Chem. Commun.* **2008**, 567.
(54) Burke, H. M.; Gunnlaugsson, T.; Scanlan, E. M. *Chem. Commun.* **2015**, *51*, 10576.

DOI: 10.1021/jacs.7b01628
J. Am. Chem. Soc. 2017, 139, 6390−6395